Structural models of amorphous silicon surfaces

G. Hadjisavvas,[1] G. Kopidakis,[1] and P. C. Kelires[1,2]
[1]*Physics Department, University of Crete, P.O. Box 2208, 710 03 Heraclion, Crete, Greece*
[2]*Foundation for Research and Technology-Hellas (FORTH), P. O. Box 1527, 711 10 Heraclion, Crete, Greece*
(Received 12 December 2000; revised manuscript received 16 March 2001; published 10 September 2001)

Using Monte Carlo simulations within the empirical potential approach, we predict and analyze possible models of the surface structure of amorphous silicon. This is a fundamental problem about which knowledge is incomplete. We address the central question regarding the dominant type of nontetrahedral atoms at the surface. Our investigations lead to two markedly different models of the surface structure. One of the models exhibits a surface layer terminated by threefold- and fourfold-coordinated atoms. In general, threefold atoms are on top and form mostly dimers and chainlike structures. The other model requires that the surface is terminated by fourfold atoms and by fivefold atoms assembled in clusters of pyramidal shape, with both types of geometries heavily distorted. We also use the tight-binding method to calculate the electronic density of states of these two possible models. The electronic fingerprints of the nontetrahedral atoms within and near the energy gap region are quite different. This distinguishes clearly the two models and could guide experimental work to infer the microscopic picture of clean amorphous silicon surfaces.

DOI: 10.1103/PhysRevB.64.125413 PACS number(s): 68.35.Bs, 61.43.Dq, 71.23.Cq, 73.20.At

I. INTRODUCTION

Knowledge about the surface structure of covalently bonded amorphous semiconductors is important for the understanding of growth mechanisms and deposition processes, since these are determined by the mobility of atoms in the near-surface environment. The central issue concerns the way that atoms at the surface discontinuity relax and reconstruct to relieve the energy cost due to their missing neighbors. This is also the central problem for crystalline surfaces, but the issues are more complicated in the amorphous case because of the presence of a high degree of structural disorder and the loss of orientational symmetry. Even in the case of amorphous silicon (*a*-Si), the most extensively studied amorphous semiconductor, knowledge about the surface structure is incomplete.

Contrary to carbon that has the possibility to display a variety of bonding hybridizations (sp^1, sp^2, and sp^3), silicon naturally can only form single σ bonds in the sp^3 configuration. So, it is not surprising that the *a*-C network is a mixed phase of all three hybridizations, depending on density, and that its surface has a tendency to form graphitelike sp^2 bonding arrangements.[1,2] In the *a*-Si network, however, any deviation in the bulk from fourfold coordination constitutes an intrinsic defect. Common sense dictates that the surface layer is a natural place, and a nucleation center, for overconcentration of atoms with non-fourfold coordination. The crucial task is to clearly distinguish in the nontetrahedral atoms those that form the natural reconstruction of the surface. Such atoms cannot be considered as defects with the usual meaning that we give to the bulk intrinsic defects. A first naive picture of the unrelaxed amorphous surface would require many undercoordinated atoms in the plane terminating the bulk network, most of them twofold coordinated. These would act as defects producing a large number of electron surface states in the energy gap of the material. The reconstruction of this terminal layer is expected to lower the surface energy and remove the excessive number of defect states from the gap.

The widely accepted model for the structure of *a*-Si is the continuous random network (CRN) model proposed originally by Polk.[3,4] In a random network structure the number of nearest neighbors of every atom is such that satisfies the atom's chemical valence. Thus, for *a*-Si the Polk model requires that each atom has four neighbors arranged in a tetrahedral sp^3 geometry. Bond lengths are distributed about their crystalline values with deviations of a few percent from the average value. Similarly, bond angles are distributed about the tetrahedral angle with average deviations of $\sim \pm 10°$. Randomness in the network results from a statistical distribution of dihedral angles. Deviations from the CRN model are a long-standing issue in the field of amorphous semiconductors, and discussions about the intrinsic defects in *a*-Si have been quite controversial.

The experimental signature of the intrinsic defect in *a*-Si is the hyperfine line-splitting observed in electron spin resonance (ESR) measurements, arising from the interaction of an unpaired electron spin with a ^{29}Si nuclear spin.[5] The interpretation of this experimental fact, regarding the origin of the ESR signal, is a matter of strong debate. The original idea is that the hyperfine splitting is produced by the unpaired electron spin localized on a threefold-coordinated atom, most commonly referred to as a ''dangling bond'' (DB).[6] An alternative interpretation was given by Pantelides who proposed[7] that the ESR signal could as well be explained by the existence of fivefold-coordinated atoms, called ''floating bonds'' (FB) due to their expected less localized wave functions, and who gave arguments that the FB could also explain the measured defect diffusion activation energies in hydrogenated *a*-Si.[8] Related experimental work gave support to this possibility,[9,10] assuming significant localization on one of the atoms, but the vast majority of experimental work up to-date interprets the ESR signal as a DB with backbond weakening.[11]

On the other hand, every theoretical simulational work on

a-Si that we know of, independently of the energy functional used to describe the interatomic interactions, predicts the existence of both types of native defects, the relative ratio of them being varied from case to case. Using Monte Carlo simulations and two well known empirical potentials[12,13] Kelires and Tersoff suggested[14] that the dominant native defect is the FB, being more numerous than the DB, because it has a lower formation energy in the *a*-Si network. Other simulations based on empirical potentials also consistently find more FB's than DB's.[15–17] Simulations based on a recently introduced empirical potential[18,19] find practically only FB's.[20] Quantum-mechanical simulations of varying accuracy also predict the presence of FB's.[21,22] Even the most accurate *ab initio* simulational approach, the Car-Parrinello molecular dynamics technique,[23] produces a considerable fraction of FB's in the amorphous network.[24] An effort was made to decide between the two possible candidates for the ESR active defect by calculating the hyperfine splittings with tight-binding calculations,[25,26] but the results are not conclusive.

As the issue stands now and in order to be fair to both points of view we could say that, independently of whether dangling or floating bonds are the ESR active centers, there are *in principle* two possible structural deviations from local tetrahedral geometry in *a*-Si. Following this reasoning, we attempt in this paper to investigate the surface structure of *a*-Si and shed some light into its reconstruction, identifying the local configurations that prevail on the surface. We examine the influence that surface geometries have on the electronic density of states (EDOS), especially in the band-gap region near the Fermi level. The nature of gap states will allow us to check whether different nontetrahedral surface geometries can be identified and distiguished. Such information is useful in order to guide experimental efforts for a fundamental microscopic study of *a*-Si surfaces, that is presently lacking. For this purpose, we do a comparative study of different structural models prepared and/or relaxed with three well known empirical potentials, and we calculate their EDOS within the tight-binding scheme.

At present, we concentrate on a detailed analysis of the surface structure of clean *a*-Si. We consider the understanding of the elemental system vital before addressing the surface properties of hydrogenated amorphous silicon, *a*-Si:H, for various reasons. For example, there is a need to elucidate the characteristics of nontetrahedral configurations near the surface discontinuity, since hydrogen incorporation or evolution is taking place *via* this environment. A better understanding of the nature of such configurations will help to approach the issue in *a*-Si:H, where the role of defects is still unclear. Also, the pure surface provides a crucial and probably better benchmark, compared to bulk calculations, for the identification of the possible non-fourfold coordinations.

We have found only two previous simulations of *a*-Si surfaces in the literature. Kilian *et al.*[27] used a method[28] incorporating a non-self-consistent version[29,30] of density functional theory within the local density approximation, and tight-binding-like local atomic orbitals to expand the wave function. They created a surface model starting from the Wooten-Waire-Winer[31] (WWW) 216-atom cell of *a*-Si, as relaxed by Fedders *et al.*,[22] by removing the periodicity in one dimension. They found that the surface consists of a mixture of threefold and fivefold atoms, with threefold atoms being more numerous, but they did not actually focus on the specific reconstruction of the surface. They considered the surface region as being the layer with thickness 5.3 Å below the top atom. This is a large portion of the size of the 216-atom cell, and so surface and bulk behavior are mingled up. We address these points by making a clear analysis of the spatial distribution of atoms with different coordination as a function of depth, from the topmost surface atoms to the inner regions of our cells. There is also a recent work that reported preliminary studies of the problem.[32] We discuss some of its conclusions below.

II. METHODOLOGY

We treat the interatomic interactions in the *a*-Si networks in two levels of accuracy. For the generation of the amorphous structures we use the empirical potential approach. This is in principle less accurate than using *ab initio* or tight-binding approaches due to the lack of quantum-mechanical description. On the other hand, advantages of this method are the simplicity, the much greater statistical precision, and the use of larger cells, which compensate in part the sacrifice in accuracy. This is important in the present case where we need large cells, deep enough to separate surface and bulk behavior. For the calculation of the electronic properties and the EDOS of the structural models produced with the first approach, we use the tight-binding method.

Our aim is to uncover the general trends in the qualitative description of surface geometries, and their corresponding EDOS, and so to distinguish betweeen possible surface reconstructions. We make a comparative study of different surface structural models produced by three well-known empirical potentials. The two of them, Tersoff's[33] and Stillinger and Weber's,[13] have been extensively used in the literature. They possess well known strengths and weaknessess. The third potential has been recently introduced by Bazant and Kaxiras[18] and co-workers.[19,20] This potential is termed EDIP (environment-dependent interatomic potential). It retains in a large extent the functional form of the SW potential, like the two-body term and the radial function of the three-body term, but with several modifications to account for changes in the local atomic environment. It is reported that it can produce a high quality *a*-Si bulk structure by direct quenching from the liquid phase,[20] contrary to the SW potential which produces a reasonable structure only after artificially strengthening the three-body interaction during the quench.[34] There are three parametrizations of the Tersoff potential for Si. We use the third one (T3) that describes the elastic properties of Si reasonably accurately. In their study[14] of *a*-Si Kelires and Tersoff used the second parametrization, which gives however a not as good description of the elastic constants. We have checked that the main conclusion of that work, namely that FB's have lower formation energies than DB's, is still valid with T3.

The present investigations are based on continuous-space Monte Carlo (MC) simulations. The underlying statistical en-

semble is the isobaric-isothermal (N,P,T) ensemble, in which equilibration of a given structure is performed under conditions of constant number of atoms N in the system, constant pressure P, and constant temperature T. These conditions are the most appropriate as they mimic usual experimental conditions in the laboratory. The implementation of this ensemble for MC simulations is done through the Metropolis algorithm.[35] We have two types of moves: random atomic displacements $(s^N \rightarrow s'^N)$, where s^N is symbolic for the $3N$ scaled atomic coordinates in the cell, and volume changes $V \rightarrow V'$. These moves are accepted with a probability

$$P_{\mathrm{acc}} = \min[1, \exp(-\beta \Delta W)] \sim e^{-\Delta W / k_B T}, \tag{1}$$

where

$$\Delta W = \Delta U_{\mathrm{displ}}(s^N \rightarrow s'^N) + P(V' - V) - N k_B T \ln(V'/V). \tag{2}$$

$\Delta U_{\mathrm{displ}}$ is the change in potential energy due to the atomic displacements both during the random moves and the volume changes. The volume involving terms (the last two terms) operate only during the volume changes.

We use two different procedures for the generation of the amorphous networks. The first approach is direct quenching from the melt. This is the most commonly used simulational method for the generation of amorphous semiconductor structures due to its simplicity. The networks formed this way can simulate *a*-Si structures prepared in the laboratory by the method of laser quenching,[36] despite that the quenching rates used in the simulations are much faster than in the experiment. Because of the fast quenching rates, it has been often argued that the production of fivefold defects during the simulations is an artifact of the liquid quench method. In other words, the overcoordinated liquidlike local geometries freeze into the supercooled glassy structure when rapidly passing through the glass transition temperature during the quench (let us recall that the liquid has an average coordination number of ~ 6.4). This argument can only be used to explain the *excessive* number of defects in the network. It is not valid in general because FB's are also generated when relaxing/annealing ideal tetrahedral CRN models (see below) with either empirical or *ab initio* methods.

In the liquid quench method the networks are generated in the following way: we start with a crystalline slab supercell of 750 atoms with two free surfaces. Periodic boundary conditions in the lateral directions are applied to the cell. The initial configuration is liquified and equilibrated at 3000 K. A number of amorphous networks are formed by quenching this liquid structure to 300 K with cooling rates up to ~ 185 (MC steps)/atom K. During melting and quenching the slab supercells are put under slight pressure (~ 300 bars) to contain the liquid. After quenching the pressure is removed and the cell densities are equilibrated.

We would like to completely bypass the problem of the fast/slow quenching rates in the simulations and the associated with it density of defects. Instead, we wish to concentrate our attention to the issue of the instability of the tetrahedral amorphous structure in the presence of the surface discontinuity. For this purpose, we follow a second procedure to generate the *a*-Si surface networks, in the same way used earlier by Kilian *et al.*[27] We start with the WWW model[31] of *a*-Si, which is a completely tetrahedral network constructed from the diamond lattice by a bond-switching mechanism. We use both 512-atom and 4096-atom cells to check for size effects. The latter cells are much larger than those used before,[27] and are thick enough to separate surface from bulk behavior. These specific bulk WWW cells have been constructed by Djordjević *et al.*[37] To form the surface environment we remove the periodicity in one dimension, going from an infinite bulk to an infinite slab. (Actually, the cells are also periodic in the third direction, but a vacuum region on top and below is introduced, which is thick enough so that atoms on the top do not interact with atoms on the bottom). This creates many twofold- and threefold-coordinated atoms on the two as-formed surfaces because of the missing neighbors. The cells are then relaxed using the empirical potentials by heating them up to 800 K and subsequently cooling them slowly to 300 K. The annealing provides the necessary energy for the atoms on the surfaces to rebond and reconstruct. In both the quenched slabs and the WWW slabs we retain the two surfaces for improved statistics, instead of fixing the atoms in the ''bottom.'' In what follows, the reported properties are averaged over the two surfaces, except where it is noted otherwise.

The cutoff distances for identifying the first nearest neighbors and thus the different coordinations are extracted from the pair distribution functions $g(r)$ calculated with the three potentials at 300 K (not shown). The maximum Si-Si bond lengths are equal to the first deep minimum in the $g(r)$. For all three potentials there is a well defined region where $g(r)$ is zero, and the cutoff distance is taken to be in the middle of that. It ranges between 2.85–2.9 Å. Only rarely an atom can fluctuate from a threefold, or a fivefold, to a fourfold character and *vice versa*. The vast majority of nontetrahedral atoms are well defined.

For the study of the electronic structure of the amorphous surface models that are produced by the empirical potentials, we carry out static tight-binding calculations. Specifically, we use the environment-dependent tight-binding potential for Si of Wang, Pan, and Ho,[38] which goes beyond the two-center approximation and allows the tight-binding parameters to scale according to the bonding environment. In this way the effects of nonorthogonality and multicenter interactions are effectively introduced. The parameters were determined by fitting to the electronic band structures and the cohesive energy versus volume curves of various bulk structures of Si. For the calculations to be feasible, we use the WWW surface models with 512 atoms and the quenched surface models with 750 atoms.

III. RESULTS AND DISCUSSION

A. Structure and energetics

1. WWW-formed cells

We first examine the surface models generated from the WWW bulk models by effectively removing the periodicity

TABLE I. Relaxation-reconstruction energetics of the surface layer and of the inner bulk portions of the "cleaved" 4096-atom WWW cells using the T3, SW, and EDIP potentials. Energies are in eV/atom.

	T3	SW	EDIP
Unrelaxed surface	−3.872	−3.802	−3.990
Relaxed surface	−3.987	−3.983	−4.228
ΔE^{surf}	−0.115	−0.181	−0.238
Unrelaxed bulk	−4.398	−4.386	−4.441
Relaxed bulk	−4.404	−4.397	−4.444
ΔE^{bulk}	−0.006	−0.011	−0.003

in one dimension. In this process, there is a significant gain in energy when the network relaxes and reconstructs, especially near the surface. To probe the surface energetics and separate it from that of the bulk, we rely on the concept of local atomic energies. As shown previously,[14,39] the empirical formalism embodied in the T3 and SW potentials allows for the decomposition of the total energy into atomic contributions. Quite similarly to the SW case, such a decomposition can be applied to the EDIP total energies. We consider the surface region as having a width of ~4 Å (the explanation for this choice and a graphical presentation is given in the following). From the atomic energies within this thin surface region we compute an average surface energy. We find an energy gain of 0.12 eV/atom when the surface reconstructs with the T3 potential, while the bulk energy gain (calculated by considering in an analogous way the bulk, inner atoms) is only 6 meV/atom. This shows that the relaxation-reconstruction is confined in the surface region. For the SW potential the surface energy gain is somewhat larger, while the EDIP potential yields the largest energy gain. Table I lists the relevant values calculated using the 4096-atom cells. The 512-atom cells give similar results. For all three potentials the bulk energy is ~−4.4 eV/atom, 0.2 eV/atom higher than the crystalline cohesive energy.

Another way of looking at the process is to analyze the distributions of atomic energies in the cells. A distribution of atomic energies can be generated by computing the probability density of finding the atoms in the cells having a local (atomic) energy E_i. We focus our attention to the surface region where the relaxation effect is maximal. Figure 1 shows the resulting distributions of the atomic energies within the thin surface layers of the 4096-atom cells using the three potentials, both before allowing surface relaxation, i.e., for the as-formed surfaces, and after surface relaxation and reconstruction. (Analysis of the corresponding distributions from the 512-atom cells shows exactly the same trends with only minor modifications, mainly in the intensity of the peaks.)

The initial spectrum is similar in all three cases. It consists of a high probability peak at the low-energy end, at ~−4.4 eV, which arises mainly from fourfold atoms in the thin layer, of a peak at the high-energy end, higher than −3 eV, arising from twofold-coordinated atoms that are artificially formed by the removal of periodicity, and of a middle wide-spread peak arising mainly from configurations

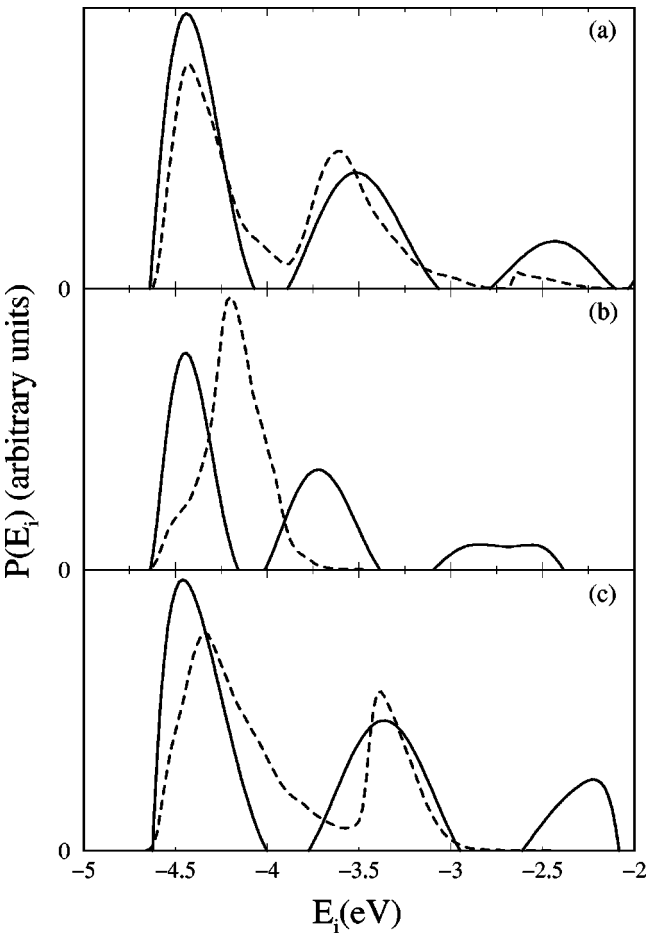

FIG. 1. Probability distributions of atomic energies in a thin surface layer having a width of 4 Å prior (solid lines) and after (dashed lines) relaxation-reconstruction, calculated using the (a) T3, (b) EDIP, and (c) SW potentials. In all three cases, 4096-atom slab cells generated from the WWW bulk models are used.

involving threefold atoms (the latter are also formed by the removal of periodicity). There are no fivefold atoms contributing to the distributions at this stage.

In the final spectrum of energies, following relaxation and reconstruction, the common characteristic in all cases is the (almost) disappearance of the twofold-atom peak, since such nontetrahedral coordinations have too high atomic energies to be stable ingredients of the surface. There are, however, significant differences regarding the other two peaks. In the T3 case, the fourfold peak widens and becomes less intense, while its position remains unaltered. The threefold peak becomes more intense and is slightly shifted to lower values. In the gap between the two peaks, observed initially before relaxation, energy states now appear that are mainly due to heavily distorted fourfold atoms. In the SW case, a similar situation occurs with the two peaks retaining their distinct nature, though the fourfold peak is more widened and shifted to higher values, and the threefold peak is more sharpened. The energy states in the gap are due to heavily distorted fourfold atoms, but also due to some fivefold atoms created by the reconstruction.

The remarkable finding in the EDIP case is the merging of the two peaks into one broad, single peak centered at ~ -4.2 eV, considerably higher than the peak energies of regular fourfold geometries in the network. This effect is the result of the generation of numerous fivefold atoms in the surface region (details are given below) that are strongly mixed up with distorted fourfold surface geometries, while the threefold atoms disappear. This indicates a major rearrangement at the surface, and it is consistent with the finding that the EDIP potential yields the largest surface energy gain. Note that the presence of the environment-dependent terms in the EDIP potential produces a more continuous distribution of energies when geometries with different coordination interact.

The interpretation of the above results, based on the energetics of the surface reconstruction, becomes more transparent and visualized by the graphical inspection of the models and the associated coordination statistics. Ball and stick representations of the three different slab models produced by the T3, EDIP, and SW potentials are portrayed in Figs. 2, 3, and 4, respectively. We display the smaller models (512 atoms) for clarity. We remind the reader that the structures have been produced by annealing at 800 K and subsequent quenching to 0 K. Both the side and top views of the slab models lead to an immediate observation: in the case of the T3 potential, primarily, and of the SW potential, in a lesser degree, the original as-formed WWW surface reconstructs into a threefold-rich network, especially in the topmost ''rough'' surface layer. The basic units in this surface network are dimers and chainlike structures composed of threefold atoms. The network connectivity is established by bonding these units to fourfold atoms that lie, in general, below the topmost threefold atoms. Rings of different sizes are found on the surface. There are some sixfold rings and many fivefold rings composed mainly of threefold atoms. There are also rings of larger size, one of them in the T3 surface being composed of thirteen atoms.

Remarkably, the picture shown by the model produced by the EDIP potential is vastly different. The surface layer is composed of fourfold and fivefold atoms, while threefold atoms are rarely found. The local geometries formed by the fivefold atoms resemble ''hat'' or ''domed'' units in which such atoms have a tendency to cluster. The topmost fivefold atoms, especially, have a quite different structure than FB's in the bulk, since they are located by necessity at the apex of the pyramidal units. Such a surface structure is unique. Previous preliminary studies by Bernstein *et al.*[32] using the EDIP potential reported such a possibility, but only for cells formed by liquid quenching. Their ''cleaved samples,'' however, formed from bulk cells by removing the periodicity in one direction, as done here, had surface regions composed of fourfold and threefold atoms, with few fivefold atoms, in apparent disagreement with our results. This discrepancy is cleared out by noting that these authors did not relax/anneal the slab cells at elevated temperatures, as we did, but they just relaxed the as-formed structures at low temperatures. Obviously, the surface is not well equilibrated this way and it is locked in the local minima of the potential. Actually, their reported structure is what we call here ''as-formed'' structure with many undercoordinated atoms [with energetics shown in Fig. 1(b), solid line]. Annealing provides the necessary energy to get out of this minima and reach the surface global minimum for the EDIP potential.

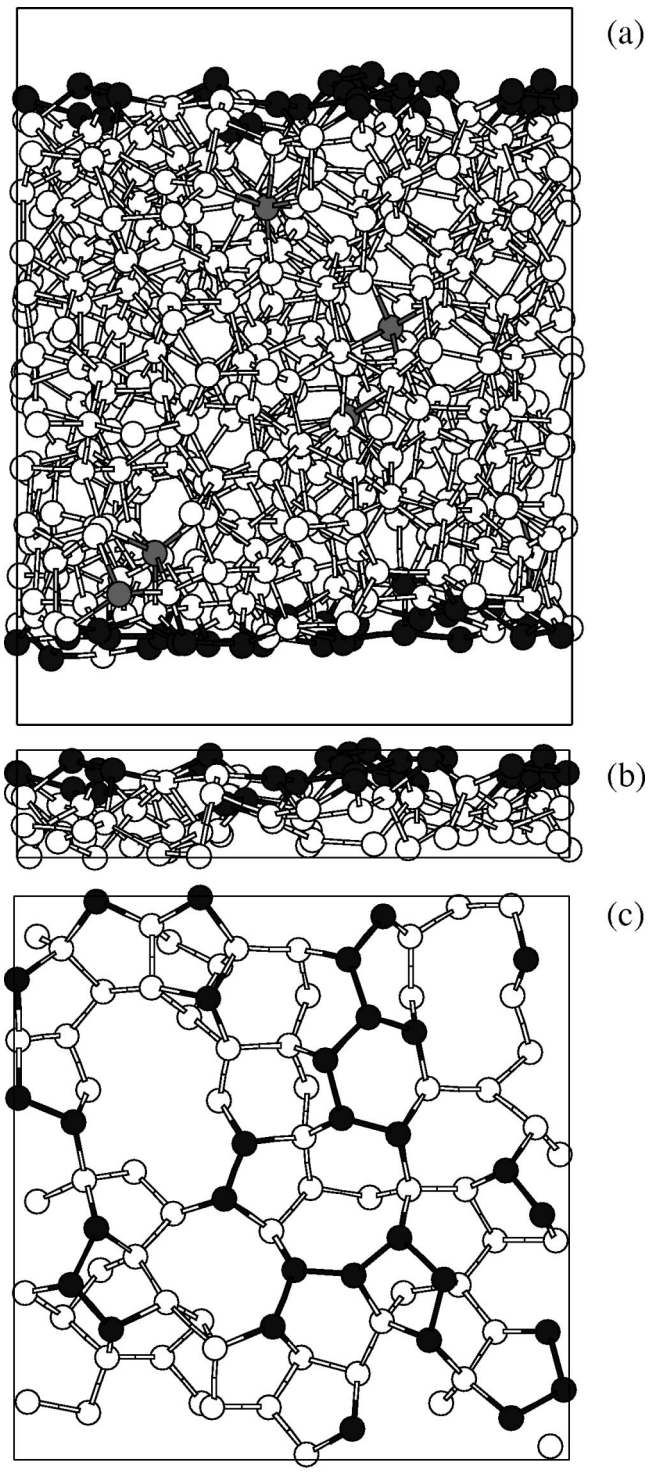

FIG. 2. Graphical representation of the 512-atom slab cell generated from the WWW bulk model using the T3 potential. Dark filled circles show threefold-coordinated atoms, gray filled circles denote fivefold atoms, and open circles show fourfold atoms. (a) Side view of the whole cell. (b) Side view of the top surface layer having a width of 4 Å. (c) View from the top of the surface layer.

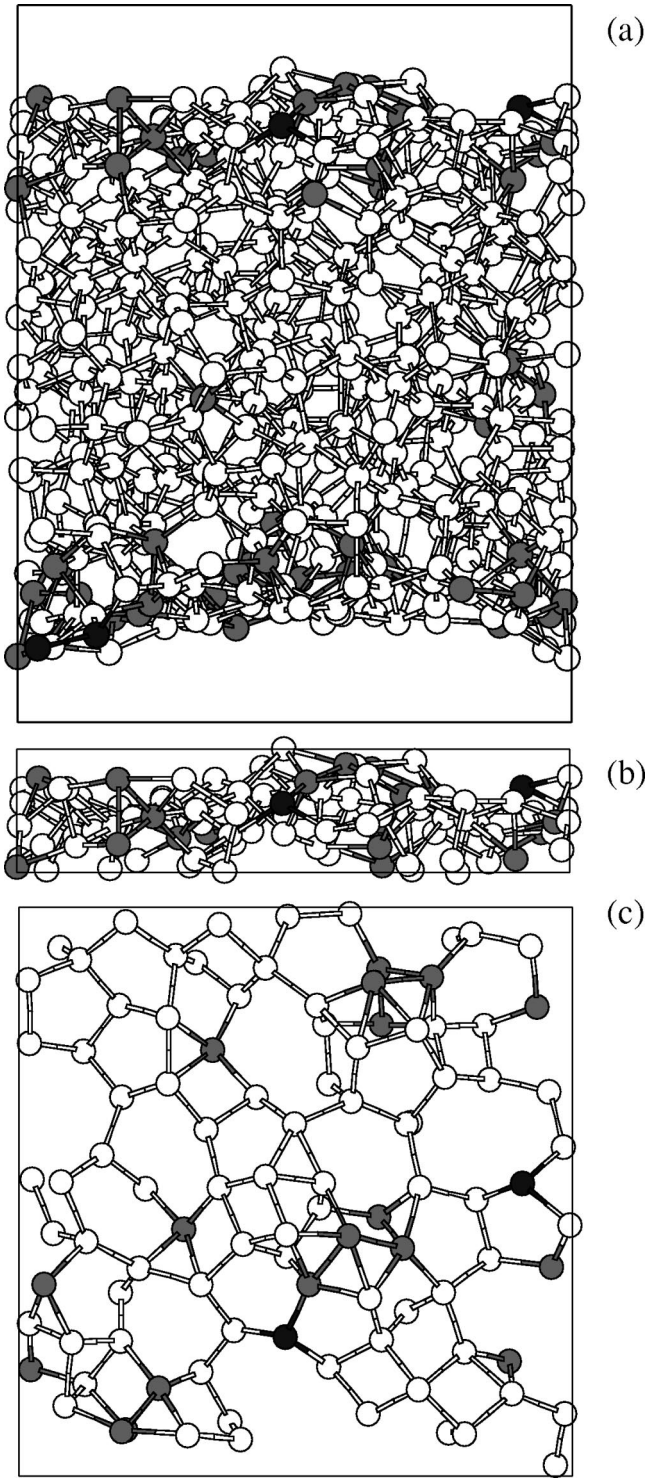

FIG. 3. Graphical representation of the 512-atom slab cell generated from the WWW bulk model using the EDIP potential. Different coordinations are denoted and panels show the same network views as in Fig. 2.

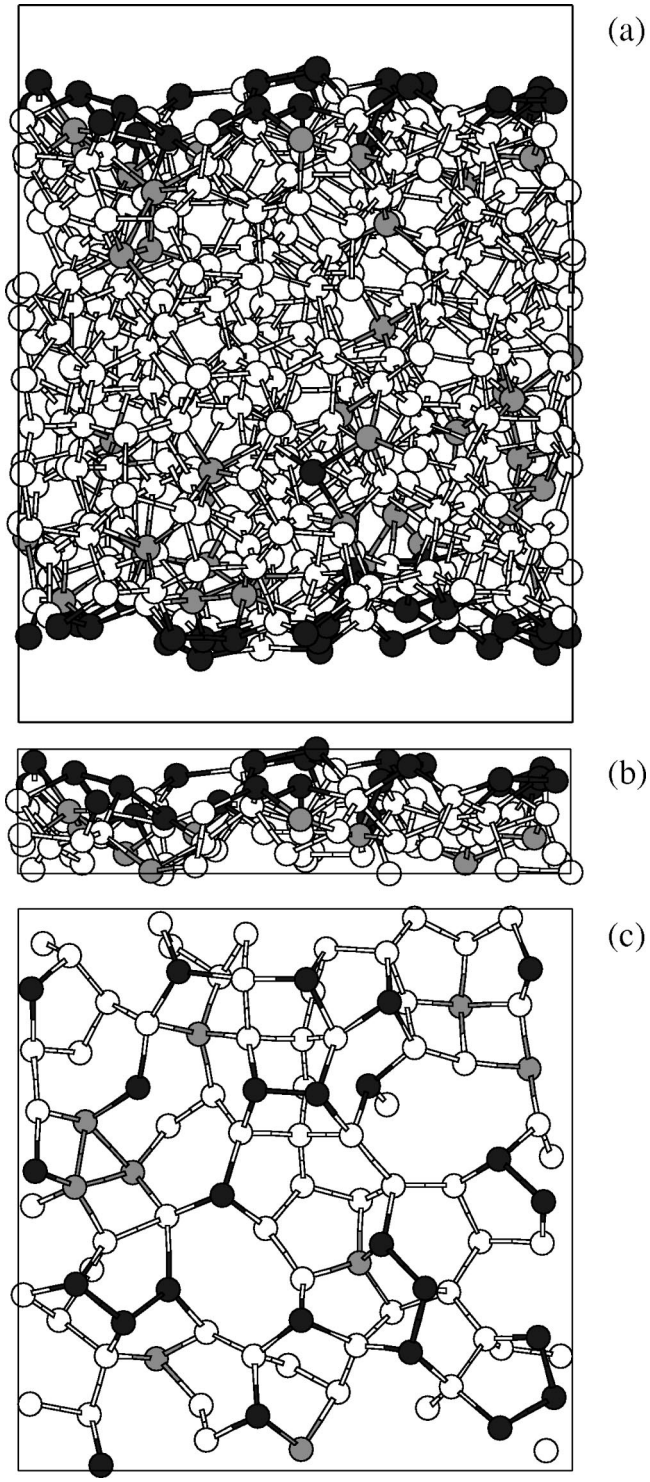

FIG. 4. Graphical representation of the 512-atom slab cell generated from the WWW bulk model using the SW potential. Different coordinations are denoted and panels show the same network views as in Fig. 2.

The coordination statistics for the three slab models (based on 4096-atom cells) are given in Table II, and along with the stick and ball representations make the distinction between the three cases clear. There are three entries for each potential in the table, namely the overall statistics in the slabs, the statistics within the thin surface layers of 4 Å (both surfaces are taken into account), and the statistics of bulk WWW models equilibrated with the three potentials for comparison with the slab models. In the T3 case, the percentage of threefold atoms in the whole slab is $\sim 7\%$ and this is

TABLE II. Coordination statistics of the 4096-atom WWW cells using the T3, SW, and EDIP potentials. For each potential there are three entries. Statistics over the whole slab cells are given in the left column. Statistics over the thin surface layers (4 Å) of the slab cells are given in the middle. Statistics over the bulk WWW cells are given in the right column.

	T3			SW			EDIP		
N_3	6.8	42.0	0.0	3.9	24.1	0.0	0.4	2.4	0.0
N_4	91.3	56.8	99.6	77.4	60.8	91.0	90.5	64.6	97.3
N_5	1.9	1.2	0.4	18.7	15.1	9.0	9.1	33.0	2.7

all found in the surface where it composes 42% of the atoms. We prefer not to name these atoms as DB's, but rather as the natural nontetrahedral coordination induced by the surface discontinuity. The percentage of fivefold atoms is ~2%. Most of them are found in the inner regions of the cell. In the EDIP case, the total percentage of fivefold atoms is ~9%. Most of these atoms (~80%) are found in the surface layer, being one third of the total number of surface atoms. In the SW case, we have an intermediate situation. In total, the percentage of threefold atoms is ~4% and they are all found in the surface, as in the T3 case, being 24% of the total number of surface atoms. The total percentage of fivefold atoms is ~19%, most of which (90%) are found in the inner regions of the cell. There is an increased percentage of fivefold atoms in the surface region (15% of the total number of surface atoms) compared to the T3 case, but still they are less than the threefold atoms and, most importantly, lie below the topmost atoms.

Among the three models, the most stable structure upon the removal of periodicity and generation of the surface discontinuity is the T3 model with 91.3% tetrahedral coordination. Slightly less stable is the EDIP model with 90.5% tetrahedral coordination. Their marked difference is in the dominant type of nontetrahedral coordination formed, the T3 favoring threefold coordination, especially at the surface, while the EDIP favors fivefold coordination. Less stable is the SW model with only 77% tetrahedral coordination.

It is interesting to compare this picture with the coordination statistics of bulk WWW models (third column of each potential entry in Table II) that have been relaxed with the three potentials at 800 K and subsequently quenched to 0 K. The prominent characteristic of this analysis is that in all three cases the percentage of threefold atoms is zero, while that of fivefold atoms is not. The observation that the relaxation of a completely tetrahedral structure, such as the WWW CRN model, results in the generation of fivefold defects leads us to conclude that the fivefold geometry is not just an artifact of the liquid quench method, as is often argued, but it rather is an intrinsic ground state property of the bulk amorphous network. Again, the most stable bulk model is the T3 structure with 99.6% tetrahedral coordination, followed by the EDIP model with 97.3%, while the SW model has a 91% tetrahedral coordination.

A nice way to show how the atoms of nontetrahedral coordinations are distributed in the slab cells, as a function of the distance z from the two surfaces, is provided by computing the position probabilities of these atoms. These are defined formally as the atomic position densities of states $P(z)=dN/dz$, where dN is the number of threefold or of fivefold sites lying in the vertical position interval between z and $z+dz$. The resulting distributions for the three models are shown in Fig. 5. The center of the slabs is taken as the origin of the z axis. It is clear that in the T3 case shown in panel (a) the probability of finding threefold atoms is sharply peaked at the surfaces, while in the EDIP case shown in panel (b) it is the fivefold probability that is peaked at the surfaces. In the SW case, we have maximum threefold probability at the surfaces, as for T3, but we also observe peaks from fivefold atoms near the surface layers. Overall, the fivefold probability in the inner parts of the cell is higher in the SW case. Figure 5 also provides us with the choice for the thickness of the surface layer (4 Å) used above. It is apparent that the thickness of the enriched with non-fourfold atoms area in both the T3 and SW cases is about 4 Å. For the EDIP, it is a bit larger, but we stick to 4 Å for consistency. None of the important conclusions reached in this subsection changes if we increase the surface layer thickness.

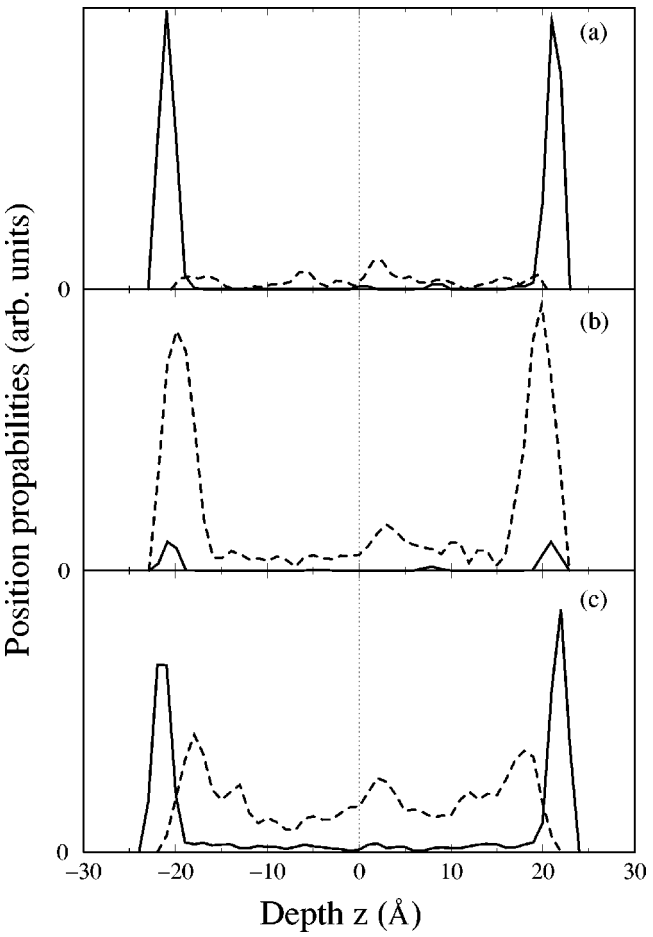

FIG. 5. Position probabilities of threefold-coordinated (solid lines) and fivefold-coordinated (dashed lines) atoms as a function of the distance from the slab center, at zero, toward the two surfaces, calculated using the (a) T3, (b) EDIP, and (c) SW potentials. In all three cases, 4096-atom slab cells generated from the WWW bulk models are used.

2. Quenched cells

As expected, the cells formed by liquid quenching contain a larger fraction of nontetrahedral atoms than the WWW-formed cells. In order to be consistent and for purposes of comparison of the structures produced using the three empirical potentials, we only prepared cells by direct quenching from the liquid to 300 K, without any further annealing. Quenching was carried out for 500 000 MC steps in all three cases, both for surface slab models as well as for bulk models. For the latter models, we found that direct quenching using the T3 potential yields 89.6% tetrahedral atoms, 0.2% DB's and 10.2% FB's. Using EDIP, we found 90.6% tetrahedral atoms, no DB's and 9.4% FB's. The fraction of tetrahedral atoms in this case is somewhat lower than the 95% reported in Ref. 20, but presumably with a slower quench this fraction will be reached. (This is not important for our discussion.) Using the SW potential, we found only 60% of atoms to be fourfold-coordinated, the rest being FB's. This was expected, since it is well known that without artificially strengthening the bond angle forces during quenching the SW potential produces a very defective amorphous structure. We therefore in the following concentrate on the T3 and EDIP quenched structures.

Despite the similarity in the bulk structures produced by T3 and EDIP, the surface models differ considerably. For T3, 83.5% of the atoms are tetrahedral, 10.5% are fivefold-coordinated and 6% are threefold-coordinated. For EDIP, the analogous fractions are 80%, 19.9%, and 0.1%, respectively. The latter potential again, as in the WWW-formed cells, produces more fivefold-coordinated and many fewer threefold-coordinated atoms than the T3 potential. More importantly, in the T3 case the vast majority of threefold atoms is concentrated on the surface, while the opposite happens in the EDIP case where the surface is heavily enriched with fivefold atoms. Side and top views of the two surface models are shown in Figs. 6 and 7. These models are very similar to the surface structures produced by the first procedure, shown in Figs. 2 and 3, and we can therefore conclude that the marked difference between the two models is independent of the generation method.

Considering the analogy with crystalline reconstructed Si surfaces, the T3 amorphous surface model is not unexpected. It involves in the top the familiar dimer pairing of undercoordinated atoms as its fundamental structural unit. On the other hand, the EDIP surface model involving in the top heavily distorted fivefold geometries is rather surprising. It seems that threefold configurations in the amorphous phase with dangling bonds pointing into the vacuum are quite costly for the EDIP potential. As pointed out above, the interesting ingredient in the EDIP picture is a fivefold atom located at the apex of a pyramidal unit composed mainly of other fivefold atoms (see Figs. 3 and 7). The angles involved in such a configuration are very different from those in a ''regular,'' bulk FB configuration where the fivefold atom is, more or less, at the center of a spherical shell. We also note that many of the fourfold atoms in the top surface layer assume similar distorted geometries deviating strongly from the tetrahedral arrangement.

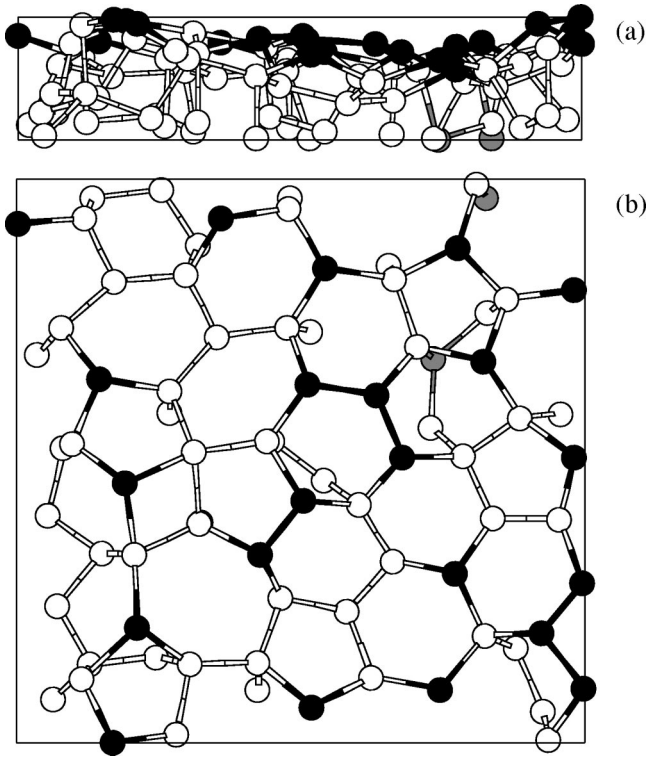

FIG. 6. Side and top views of the surface layer (4 Å width) of a 750-atom cell produced by liquid quenching using the T3 potential. Dark filled circles show threefold-coordinated atoms, gray filled circles denote fivefold atoms, and open circles show fourfold atoms.

The fundamental difference between the two pictures cannot be easily traced in the functional forms of the three empirical potentials used. The difficulty arises because the disordered amorphous environment, especially near the surface discontinuity, puts an additional burden for the comparison of parametrized potential functions that were fitted to bulk structures and their properties. It is, however, reasonable to assume that this dissimilarity is mainly attributed to the treatment of angular forces, rather than of radial forces, by each potential. While the implicit many-body character of the T3 format makes it hard to compare with the other two potentials, a comparison can be made between the SW and EDIP forms. The EDIP two-body term is quite similar to the SW form, but it is modified with an extra function to incorporate the effect of changes in the local atomic coordination on the bond strength.[20] More significant is the difference in the three-body terms, where the radial parts are the same but the angular parts are very different. The EDIP angular function is strongly dependent on the local coordination and gives a considerably weaker interaction at small angles than the SW form. It seems therefore that this strong dependence on the local coordination, that was introduced in the EDIP form to capture the transition from covalent bonding to metallic bonding, gives rise to the different response of the amorphous network to the surface discontinuity.

At this stage, neither the comparison to the crystalline case nor any energetics arguments can allow us to choose one of the two pictures as the most probable termination of a

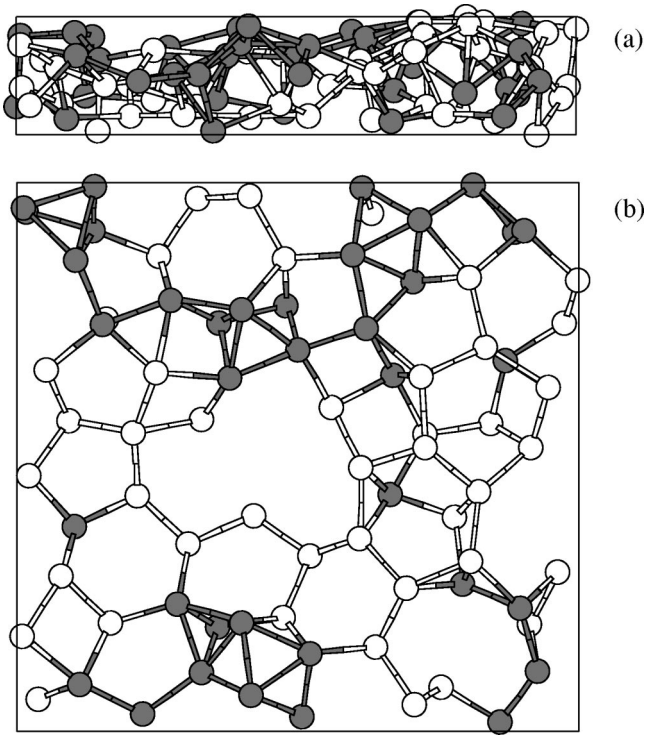

FIG. 7. Side and top views of the surface layer (4 Å width) of a 750-atom cell produced by liquid quenching using the EDIP potential. Different coordinations are denoted as in Fig. 6.

clean *a*-Si surface, given the lack of any experimental microscopic input to this matter. The work of Kilian *et al.*[27] does not shed light into this discrepancy for the reasons mentioned in the Introduction. We thus proceed to study the electronic structure of the models. This can be used as an additional probe of the surface environment.

B. Electronic density of states

The existence of two distinctly different models for the surface structure of clean *a*-Si gives us the opportunity to investigate whether there is a marked dissimilarity in their electronic properties. This can guide experimental work to distinguish between the two cases, if possible. We are mainly aiming at the identification of the electronic signatures of nontetrahedral configurations in the EDOS. Since the SW surface model is close to the T3 model, we present in the following the electronic structure of the T3 and EDIP models.

As a test of the tight-binding scheme that we use, and before addressing the surface problem, we calculated the electronic DOS of the bulk WWW models that were relaxed with the T3 and EDIP potentials, as described above. The EDOS are shown in Fig. 8. In both cases, the valence band consists of two broad regions. The low-energy region is mainly *s*-type while the high-energy broad peak is *p*-type. The conduction band is nearly featureless. The two models differ in the gap region. Expectedly, the T3-WWW model exhibits a clean gap, which is consistent with the nearly perfect tetrahedral nature (99.6%) of the network. The EDIP-WWW model, having 97.3% tetrahedral coordination, shows

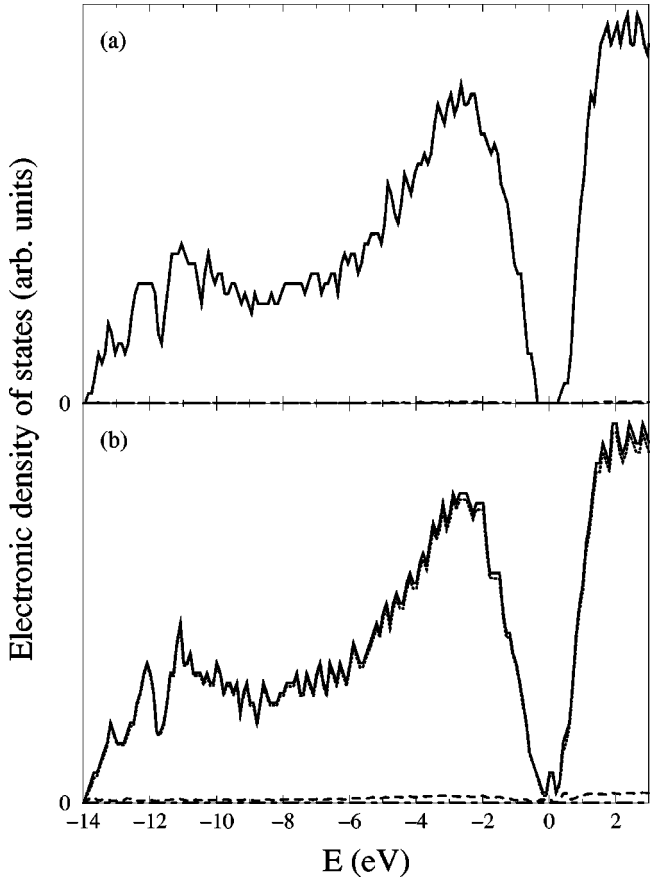

FIG. 8. Electronic density of states of the bulk WWW model relaxed with the (a) T3 and (b) EDIP potentials. The solid lines show the total EDOS. Dotted, dashed, and dash-dotted lines denote decomposition of the total EDOS into partial contributions from the fourfold-, fivefold-, and threefold-coordinated atoms, respectively.

states in the gap. The decomposition of the total EDOS into contributions according to coordination shows that these are mainly due to heavily distorted fourfold atoms rather than due to the presence of FBs (2.7%). The latter type of atoms give rise to additional states near the two band edges. We discuss this effect below. Similarly, in the T3 model, the very few FB's do not introduce any states in the gap, but deep in the valence and conduction band (they are hardly noticed).

The corresponding calculated EDOS of the WWW-formed surface models are depicted in Figs. 9 and 10 for the T3 and EDIP cases, respectively. The total EDOS are again decomposed into contributions according to coordination. The two models exhibit the same overall behavior in the valence and conduction bands, but there is a remarkable difference in the EDOS near and within the gap region. While in both cases the introduction of surface gap states is obvious, when compared to the EDOS of the ''generator'' cells portrayed in Fig. 8, the shape of the profile is distinctly contrasting. The total EDOS of the T3-WWW model exhibits peak behavior in the gap in the vicinity of the Fermi level, while the total EDOS of the EDIP-WWW model has a minimum in the gap. Let us emphasize that the excess DOS are mainly surface states because, as we showed above, the substantial modifications in the WWW models, when going

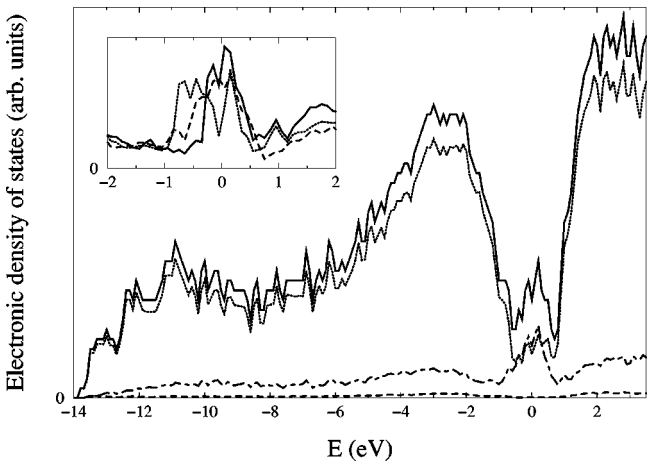

FIG. 9. Electronic density of states of the surface model generated from the WWW bulk model using the T3 potential. The Fermi energy is at zero. The total EDOS is decomposed as in Fig. 8. The inset shows the EDOS of the threefold atoms further decomposed into contributions from isolated atoms (solid line), dimers (dotted line), and chains (dashed line) within and near the band gap.

from the infinite bulk to the slab, occur in the thin surface region, and the vast majority of the nontetrahedral atoms are generated in this region.

The analysis according to coordination sheds light into the origins of this difference. The peak behavior (multiple peaks merging into one broad peak centered at the Fermi level) in the T3-WWW model originates mostly from the threefold atoms that are generated after the surface reconstruction (see Fig. 2). Most interestingly, a further decomposition of the partial EDOS of the threefold atoms into contributions according to their degree of clustering (given in the inset of Fig. 9), shows that isolated threefold atoms contribute the most to the peaked states in the gap, while pairs (dimers) and chain structures contribute less. Thus, the less ''dangling-bond'' behavior the smaller the peaked states in the gap. The

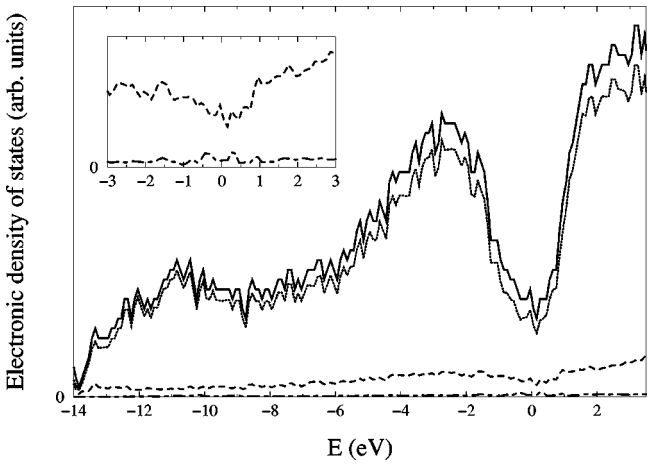

FIG. 10. Electronic density of states of the surface model generated from the WWW bulk model using the EDIP potential. The Fermi energy is at zero. The total EDOS is decomposed as in Fig. 8. The inset shows an enlargement of the region within and near the band gap, focusing on the fivefold and threefold contributions.

remaining states in the gap originate from heavily distorted fourfold atoms. Many of these atoms lie in the surface region and their distortions are associated with the strain induced by the layer of threefold atoms on top. The few fivefold atoms, that lie deeper in the slab cell, do not contribute any states in the gap.

On the other hand, the contrasting picture of the EDIP-WWW EDOS is attributed to the lack of any threefold atoms on the surface. The states in the gap originate mostly from distorted fourfold atoms and less from the fivefold atoms. In fact, the latter contribute more states deep in the top of the valence band and in the bottom of the conduction band, while the distribution has a minimum in the gap, as it is clearly depicted in the inset of Fig. 10. A further analysis of both the fourfold and fivefold distributions shows that most of the states in the gap originate from atoms in the thin surface layer than from atoms that lie deeper in the ''bulk'' portions of the slab cell.[40]

A similar analysis of the EDOS of the quenched cells shows exactly the same trends and overall behavior. Also, the SW models produce expectedly EDOS of a quite similar profile as the T3 models. We conclude that there is a universal and fundamental difference between the EDOS of the two structural models. This stems from the property of threefold-coordinated atoms to introduce peaked states in the gap near the Fermi level, and the property of fivefold atoms to induce more states at the two outer band edges, rather than within the gap. Distorted fourfold atoms also produce more gap states than fivefold atoms. These are the key findings of our investigations. This picture is in accord with the work of Knief *et al.*[26] who found a similar behavior of the nontetrahedral atoms in the bulk of *a*-Si. It is also consistent with the work of Kilian *et al.*[27] who found that most of the localized states in the gap are centered on threefold-coordinated atoms, localization is less for states centered on fourfold atoms, while states centered on fivefold atoms are delocalized.

However, there are seemingly some differences with two of the previous studies. Bernstein *et al.*[32] proposed that the electronic signatures of threefold and fivefold coordinated atoms at the amorphous surface are difficult to distinguish. This apparent disagreement with our results is explained when taking into account that these authors chose to present the excess EDOS of their two surface models (one threefold rich, the other fivefold rich) with respect to the amorphous bulk EDOS, instead of plotting the direct EDOS for each coordination. We verified that indeed this is the case by plotting the excess EDOS of our models. The difference EDOS are shown in Fig. 11. We find a very similar difference feature in the gap as found by Bernstein *et al.* Therefore, the distinct signature of the non-fourfold coordinations cannot be revealed with such analysis.

In the work of Kilian *et al.*,[27] who reported a surface model with roughly equal fractions of threefold and fivefold atoms, the EDOS do not show a midgap peak. Two possible reasons could lead to this discrepancy with our findings. Either the fivefold contribution hides the peak of the threefold atoms, or the resolution (broadening) in their EDOS washes out this feature. Note that the total percentage of fivefold atoms in their cell (4.6%) is significantly higher than ours

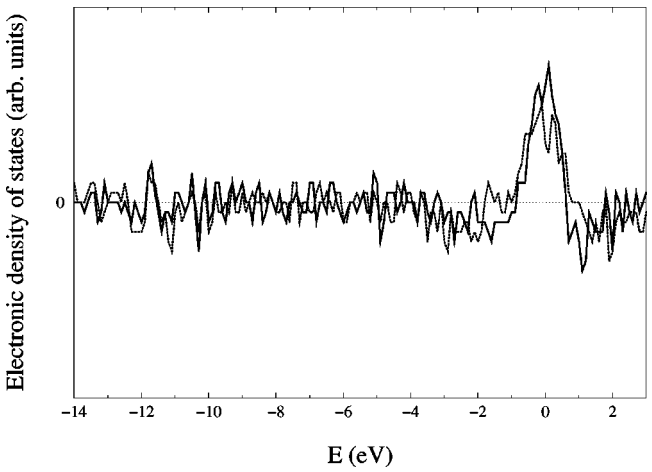

FIG. 11. Excess EDOS of the T3 (solid line) and EDIP (dotted line) surface models, plotted as the difference between the respective slab cell EDOS (portrayed in Figs. 9 and 10, respectively) and the bulk amorphous EDOS (shown in Fig. 8).

(1.9%), despite that both cells were generated in the same way (removing the periodicity in the bulk WWW cells). The fourfold network is somewhat less stable under the approximate *ab initio* method used by them (in total 10.2% nontetrahedral coordination compared to 8.7% found by us).

The different electronic signatures of undercoordinated and overcoordinated atoms at the amorphous surface, and the resulting dissimilarity of the EDOS in the gap region, can serve as a guide for careful experimental studies of the microscopic structure at the surface and its associated electronic properties. The problem is of fundamental interest. Experimental work with high resolution able to probe locally the surface environment will be very useful.

IV. SUMMARY

We have carried out in this work detailed Monte Carlo simulations within the empirical potential approach, with the purpose of addressing a fundamental problem in the field of amorphous semiconductors, that is to identify the microscopic structural properties of *a*-Si surfaces and some of the associated electronic properties. By using three well known empirical potentials we ended up at two markedly different structural models for the surface. We studied the energetics of surface formation and the details in the structural characteristics of both models, with emphasis on the question about the dominant type of atoms with nontetrahedral coordination that enrich the surface.

The first model requires that the surface of *a*-Si is terminated by threefold and fourfold atoms, with the former occupying the top positions and forming mostly dimer and chainlike local geometries. An ''as-formed'' cleaved surface, starting from the bulk, that contains many twofold-coordinated atoms is unstable and transforms upon annealing and consequent relaxation-reconstruction into this threefold-rich surface. The second model, on the other hand, requires that the surface is terminated by fivefold atoms mostly clustered in pyramidal units, as well as by fourfold atoms. The fivefold atoms in these units are heavily distorted and their topology is different from that of fivefold defects in the bulk.

We have also examined the electronic density of states associated with the two structural models using the tight-binding method. We found that the corresponding EDOS differ substantially within and near the band gap region, because the two possible nontetrahedral types of atoms have distinctive electronic signatures. The threefold surface atoms produce states in the gap forming peaks in the vicinity of the Fermi level, the intensity of which depends on the degree of clustering of threefold atoms, while the fivefold surface atoms produce an excess of states at the outer band edges and deeper in the valence and conduction bands. Experimental work that could probe the EDOS locally at the surface will be very useful to distinguish between these two possibilities.

ACKNOWLEDGMENTS

This work was supported by research Grant No. 97EΛ-52, from the Greek General Secretariat for Research and Technology.

[1] P.C. Kelires, J. Non-Cryst. Solids **227-230**, 597 (1998).
[2] J. Dong and D.A. Drabold, Phys. Rev. B **57**, 15 591 (1998).
[3] D.E. Polk, J. Non-Cryst. Solids **5**, 365 (1971).
[4] D.E. Polk and D.S. Boudreaux, Phys. Rev. Lett. **31**, 92 (1973).
[5] C. P. Slichter, *Principles of Magnetic Resonance* (Springer-Verlag, Berlin, 1980).
[6] J.C. Philips, Phys. Rev. Lett. **42**, 1151 (1979).
[7] S.T. Pantelides, Phys. Rev. Lett. **57**, 2979 (1986).
[8] S.T. Pantelides, Phys. Rev. Lett. **58**, 1344 (1987).
[9] J.H. Stathis and S.T. Pantelides, Phys. Rev. B **37**, 6579 (1988).
[10] J.H. Stathis, Phys. Rev. B **40**, 1232 (1989).
[11] M. Stutzmann, M.S. Brandt, and M.W. Bayerl, J. Non-Cryst. Solids **266-269**, 1 (2000).
[12] J. Tersoff, Phys. Rev. B **37**, 6991 (1988).
[13] F. Stillinger and T. Weber, Phys. Rev. B **31**, 5262 (1985).
[14] P.C. Kelires and J. Tersoff, Phys. Rev. Lett. **61**, 562 (1988).
[15] M.D. Kluge, J.R. Ray, and A. Rahman, Phys. Rev. B **36**, 4234 (1987).
[16] W.D. Luedtke and U. Landman, Phys. Rev. B **40**, 1164 (1989).
[17] R. Biswas, G.S. Grest, and C.M. Soukoulis, Phys. Rev. B **36**, 7437 (1987).
[18] M.Z. Bazant and E. Kaxiras, Phys. Rev. Lett. **77**, 4370 (1996).
[19] M.Z. Bazant, E. Kaxiras, and J.F. Justo, Phys. Rev. B **56**, 8542 (1997).
[20] J.F. Justo, M.Z. Bazant, E. Kaxiras, V.V. Bulatov, and S. Yip, Phys. Rev. B **58**, 2539 (1998).
[21] D.A. Drabold, P.A. Fedders, O.F. Sankey, and J.D. Dow, Phys. Rev. B **42**, 5135 (1990).
[22] P.A. Fedders, D.A. Drabold, and S. Klemm, Phys. Rev. B **45**, 4048 (1992).

[23] R. Car and M. Parrinello, Phys. Rev. Lett. **55**, 2471 (1985).
[24] I. Stich, R. Car, and M. Parrinello, Phys. Rev. B **44**, 11 092 (1991).
[25] R. Biswas, C.Z. Wang, C.T. Chan, K.M. Ho, and C.M. Soukoulis, Phys. Rev. Lett. **63**, 1491 (1989).
[26] S. Knief and W. von Niessen, Phys. Rev. B **60**, 5412 (1999).
[27] K. Kilian, D.A. Drabold, and J.B. Adams, Phys. Rev. B **48**, 17 393 (1993).
[28] O.F. Sankey and D.J. Niklewski, Phys. Rev. B **40**, 3979 (1989).
[29] J. Harris, Phys. Rev. B **31**, 1770 (1985).
[30] W. Foulkes and R. Haydock, Phys. Rev. B **39**, 12 520 (1989).
[31] F. Wooten, K. Winer, and D. Weaire, Phys. Rev. Lett. **54**, 1392 (1985).
[32] N. Bernstein, M.J. Mehl, D.A. Papaconstantopoulos, N.I. Papanikolaou, M.Z. Bazant, and E. Kaxiras, Phys. Rev. B **62**, 4477 (2000).
[33] J. Tersoff, Phys. Rev. B **38**, 9902 (1988).
[34] W.D. Luedtke and U. Landman, Phys. Rev. B **37**, 4656 (1988).
[35] N. Metropolis, A.W. Rosenbluth, M.N. Rosenbluth, A.H. Teller, and E. Teller, J. Chem. Phys. **21**, 1087 (1953).
[36] S. Roorda, W. Sinke, J. Poate, D. Jacobson, S. Dierker, B. Dennis, D. Eaglesham, F. Spaepen, and P. Fuoss, Phys. Rev. B **44**, 3702 (1991).
[37] B.R. Djordjević, M.F. Thorpe, and F. Wooten, Phys. Rev. B **52**, 5685 (1995).
[38] C.Z. Wang, B.C. Pan, and K.M. Ho, J. Phys.: Condens. Matter **11**, 2043 (1999).
[39] P.C. Kelires, Phys. Rev. Lett. **68**, 1854 (1992).
[40] Note that in the calculation of the EDOS both surfaces of the slab cells are taken into account. Therefore, upon normalization the density of the gap states will be reduced.